PRESENTATION TITLE

Evaluation of surrogate signals derived from MR images to build respiratory motion models

AUTHOR(S)

Elena H. Tran[1*], Björn Eiben[1], Andreas Wetscherek[2], Uwe Oelfke[2], Gustav Meedt[3], David J. Hawkes[1], and Jamie R. McClelland[1]

[1] *Medical Physics and Biomedical Engineering, University College London, London, UK*
[2] *Joint Department of Physics, The Institute of Cancer Research and The Royal Marsden NHS Foundation Trust, London, UK*
[3] *Elekta, Medical Intelligence Medizintechnik GmbH, Schwabmuenchen, Germany*

ABSTRACT

Purpose: An MRI-Linac can provide real-time imaging during treatment delivery, but the image data is limited to a few 2D slices. Surrogate-driven respiratory motion models could be used to estimate the motion of the rest of the anatomy from the real-time images. In this study, we evaluated several surrogate signals that are derived from MR images and could potentially be used on an MRI-Linac.

Materials & Methods: Interleaved sagittal cine-MR images from two slice locations through the tumour volume were acquired from 6 lung cancer patients. Images from one slice location were used to generate surrogate signals (surrogate images), images from the other location were used to build and evaluate the motion models (model images). Surrogate signals were generated by measuring diaphragm and skin surface motion, and by applying Principal Component Analysis (PCA) to the image intensities and to the deformation fields (DFs) resulting from the group-wise registration of the surrogate images. The surrogate signals were interpolated at the timepoints of all model images (Fig. 1). Group-wise registration was also performed on the model images to obtain motion measurements as DFs, representing the motion relative to the average image obtained from the registration.
Each dataset was divided in half, with the first half (~60 model images) used for building the models and the second half for testing them. Different combinations of surrogate signals were used to fit linear correspondence models. The models were fit to the DFs from either 10 or 5 training images from the building set (Fig. 1). Thus, six different sets of training images could be selected, enabling 6-fold cross validation to investigate the robustness of the models. The small number of training images approximates the amount of data that would be available if the model slices were from a multi-slice acquisition covering the whole anatomy rather than a single slice. The deformation field error (DFE) is the difference between the DFs estimated by the models and the registration results, and was computed for each image of the test set.

Results: Table 1 reports the summary statistics of the L2 norm of the DFE over all cross-validations and patients, for each of the surrogate signal combinations investigated, for both 5 and 10 training images. The mean, standard deviation (std) and 95th percentile values were calculated over all pixels within the body, averaged over all test images. Using the scores of the first two Principal Component (PC) from DF as surrogate signals resulted in the lowest statistical values. Good results are obtained when using 10 training images, but the results are less good when using 5 training images.

Conclusions: We have developed and evaluated several promising MRI-derived surrogate signals, and found that applying PCA to the DFs from the surrogate images gave the best results. We also found that using 10 training images gave noticeably better results than using only 5. These findings will help inform our future work on 3D motion models from multi-slice acquisitions, which can ultimately be used to guide adaptive RT on an MRI-Linac.

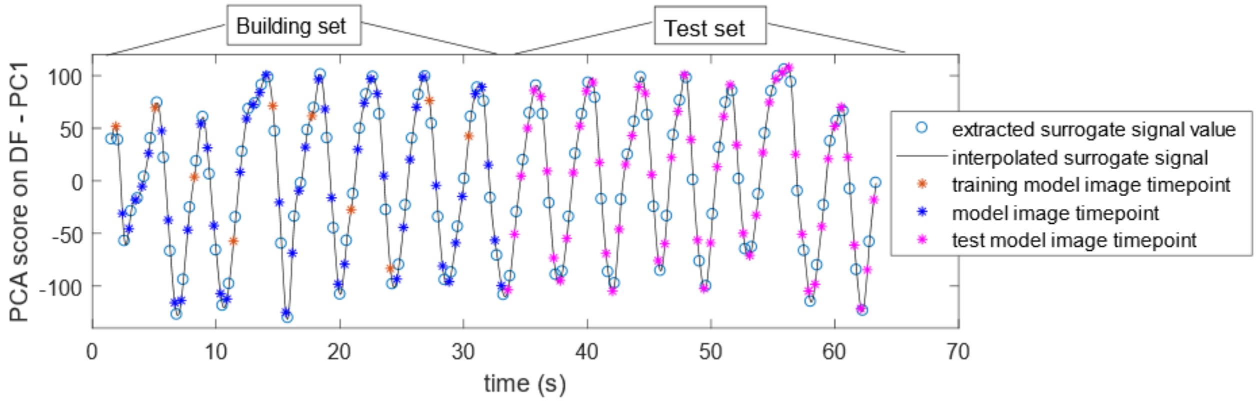

Figure 1. Example of respiratory surrogate signal for one patient. The surrogate signal is given by the scores of the first PC from the DF. The 10 training model images are used to fit the model for the first cross-validation.

	10 TRAINING IMAGES			5 TRAINING IMAGES		
SURROGATE SIGNALS	MEAN	STD	95^{th}%TILE	MEAN	STD	95^{th}%TILE
Scores of the 1^{st} PC on DF + its temporal derivative	0.75	0.72	2.20	0.90	0.89	2.69
Scores of the 1^{st} PC on intensities + its temporal derivative	0.79	0.77	2.35	0.94	0.91	2.79
Diaphragm signal + its temporal derivative	0.81	0.76	2.33	0.99	0.94	2.88
Skin signal + its temporal derivative	0.99	0.96	2.95	1.21	1.22	3.68
Diaphragm signal + skin signal	0.79	0.76	2.32	0.97	0.94	2.87
Scores of the 1^{st} PC + 2^{nd} PC on DF	0.73	0.70	2.13	0.90	0.87	2.64
Scores of the 1^{st} PC + 3^{rd} PC on DF	0.80	0.76	2.29	1.02	0.99	2.97
Scores of the 1^{st} PC + 2^{nd} PC on intensities	0.78	0.74	2.25	1.00	0.96	2.88
Scores of the 1^{st} PC + 3^{rd} PC on intensities	0.77	0.74	2.26	1.04	0.99	3.05
Diaphragm signal + its temporal derivative + skin signal	0.86	0.84	2.54	1.44	1.48	4.40
Scores of the 1^{st} PC + 2^{nd} PC + 3^{rd} PC on DF	0.78	0.75	2.28	1.20	1.20	3.60
Scores of the 1^{st} PC + 2^{nd} PC + 3^{rd} PC on intensities	0.76	0.74	2.24	1.35	1.35	4.04
No motion model	1.39	1.09	3.62	1.39	1.09	3.62

Table 1. Summary statistics of the L2 norm of the DFE for different motion models using different surrogate signals and number of training images. The statistics are averaged over all cross-validations and patients, and are given in mm.